

See discussions, stats, and author profiles for this publication at: <https://www.researchgate.net/publication/377265206>

# Numerical modeling of volumetric behavior of unsaturated expansive soil under wetting and drying cycles

Conference Paper · October 2023

CITATIONS

3

READS

224

4 authors:



**Milad Jabbarzadeh**

Sharif University of Technology

8 PUBLICATIONS 20 CITATIONS

SEE PROFILE



**Saeed Turchi**

University of Luxembourg

33 PUBLICATIONS 234 CITATIONS

SEE PROFILE



**Ali Golaghaei Darzi**

Sharif University of Technology

19 PUBLICATIONS 129 CITATIONS

SEE PROFILE



**Hamed Sadeghi**

Sharif University of Technology

88 PUBLICATIONS 1,080 CITATIONS

SEE PROFILE



# Numerical modeling of volumetric behavior of unsaturated expansive soil under wetting and drying cycles

Milad Jabbarzadeh Ghandilou<sup>1</sup>, Saeed Turchi<sup>2</sup>, Ali Golaghaei Darzi<sup>3</sup>, Hamed Sadeghi<sup>4</sup>

1- M.Sc. Student, Department of Civil Engineering, Sharif University of Technology, Tehran, Iran

2- MSCA Postdoctoral Fellow, Institute of Hydrogeology, Engineering Geology and Applied Geophysics, Faculty of Science, Charles University, Prague, Czech Republic

3- Ph.D. Student, Department of Civil Engineering, Sharif University of Technology, Tehran, Iran

4- Assistant Professor, Department of Civil Engineering, Sharif University of Technology, Tehran, Iran

[hsadeghi@sharif.edu](mailto:hsadeghi@sharif.edu)

## Abstract

Expansive soils undergo volumetric changes due to moisture variations as a result of soil-atmosphere interaction. In this study, the moisture-induced volumetric changes in unsaturated expansive soil under wetting-drying cycles were modeled. The variations in moisture content during wetting and drying cycles were analyzed for a specific type of expansive soil using one-dimensional coupled hydro-mechanical analysis within the framework of the Barcelona Expansive Model for expansive soils (BExM). The modeling was performed utilizing the finite element method in CODE\_BRIGHT. The volume changes in the soil due to wetting and drying cycles, associated with changes in moisture and suction in the unsaturated zone, led to repetitive swelling and shrinkage deformations in the expansive soil. The effects of these variations were significantly more pronounced in the initial cycles, and after several cycles, the cyclic behavior within a specified range persisted for the same defined range of suction changes. However, this trend shifted towards more elastic behavior at lower rates of suction changes. Furthermore, the effect of surcharge on the volumetric behavior of swelling soil during wetting and drying cycles was investigated. As the surcharge increased, the magnitudes of cyclic deformation decreased. By comparing soil deformation under two different surcharge, elastic behavior was observed in the first three initial cycles for higher surcharge, followed by irreversible deformations. For lower surcharge, irreversible deformations were observed after the first cycle until equilibrium was reached after several wetting and drying cycles.

**Keywords:** Numerical modeling, BExM constitutive model, Volumetric behavior, Unsaturated expansive soil, Wetting-drying cycles.

## 1. Introduction

Expansive soils naturally undergo volume changes due to alterations in climatic conditions, experiencing cycles of wetting and drying. Generally, the stress and strain pathways during these cycles deviate from a simple uniform process (Alonso et al., 2005). These soils predominantly contain montmorillonite minerals, highly sensitive to moisture variations, displaying noticeable swelling and shrinkage deformations. Some swelling soils have exhibited a volume increase of up to 30% or more due to increased moisture (Qi and Vanapalli, 2015). Due to soil-atmosphere interaction in real conditions, expansive soils are exposed to solar radiation and temperature changes, changing soil moisture during evaporation or rainfalls. Consequently, these soils are highly susceptible to cracking during the desiccation process, extending both in surface and depth and changing soil moisture and temperature distribution (Jabbarzadeh et al., 2023). In addition, they tend to swell during rainfall, which can lead to geohazards such as slope instabilities (Sadeghi et al., 2023).

The extent of swelling deformation intensifies with rising water content or diminishing suction, while shrinkage deformation magnifies with decreasing water content or increasing suction. Initially, in the wetting-drying cycles, the contrast between swelling and shrinkage deformations peaks during the first cycle and

subsequently diminishes as the cycles progress. Before attaining equilibrium, the accumulated deformation (whether swelling or shrinkage) depends on soil characteristics, initial hydromechanical conditions, vertical stress, or confining pressure. Eventually, soil deformation stabilizes after a specific number of wetting-drying cycles, reaching an equilibrium state (Zhao et al., 2018). The initial structure of swelling soils changes after the first or second cycle, and repeated wetting and drying cycles cause re-aggregation and rearrangement of the soil mass structure. All experiments concerning wetting and drying cycles indicate that after several cycles, the soil reaches equilibrium and exhibits elastic behavior, which can be attributed to the reconstruction of its structure (Estabragh et al., 2014). Micro and macrostructure behavior of expansive soils under wetting-drying cycles were also investigated through numerous experimental and numerical studies (Ghandilou et al., 2023; Wen et al., 2022; Xu et al., 2022). They concluded that these two structural levels have opposite behavior during wetting and drying.

In this study the impact of wetting and drying cycles on the volumetric behavior of unsaturated expansive soils was investigated through numerical modeling using the finite element method, employing the CODE\_BRIGHT program (Olivella et al., 1996). The Barcelona Expansive model (BExM) was utilized to assess the elastoplastic behavior of soil during suction changes.

## 2. Theoretical framework of elastoplastic Barcelona Expansive Model (BExM)

Alonso et al. (1990) introduced the Barcelona Basic Model (BBM) to examine the behavior of unsaturated soils within the framework of hardening plasticity using two independent sets of stress variables: the excess of total stress over air pressure and the suction. Subsequently, Alonso et al. (1999) further developed this model, incorporating the conceptual approach of elastic deformations in the microstructure and plastic deformations in the macrostructure of expansive soils. The BExM was validated for its accuracy in predicting pure volumetric strains concerning the combined effect of vertical stress and soil suction using laboratory experimental data. In essence, the BExM allows for the exploration of irreversible swelling deformations during soil drying, cumulative volumetric swelling or shrinkage during hydraulic cycles, and the soil's response to stress paths (Mrad et al., 2006).

The model involves three independent stress variables: the total mean net stress,  $p$ , which is the excess of total mean stress ( $\sigma_m$ ) over air pressure ( $u_a$ ), the suction ( $s$ ), and the deviatoric stress ( $q$ ). The BExM encompasses two distinct structural levels of expansive soils: the microstructural level, corresponding to the active clay minerals, and the macrostructural level, responsible for significant structural rearrangement. At the microstructural level, saturation is assumed, allowing the application of the effective stress concept. Volumetric and elastic microstructural strains are considered independent of the macrostructure. Thus, the linear relationship  $p + s = \text{constant}$  represents a Neutral Line (NL), where no microstructural deformations occur. This line separates the domain of microstructural swelling from the domain of microstructural shrinkage within the  $p$ - $s$  plane. Microstructural swelling influences the macrostructure's arrangement, causing an irreversible increase in void ratio ( $e$ ). Conversely, microstructural shrinkage induces an irreversible decrease in  $e$ . To model these phenomena, two additional yield loci are introduced: the Suction Increase (SI) line and the Suction Decrease (SD) line (Figure 1). These lines run parallel to the Neutral Line NL and determine the elastic region, where strains are reversible. Irreversible strains occur as the stress state intersects one of these two lines.

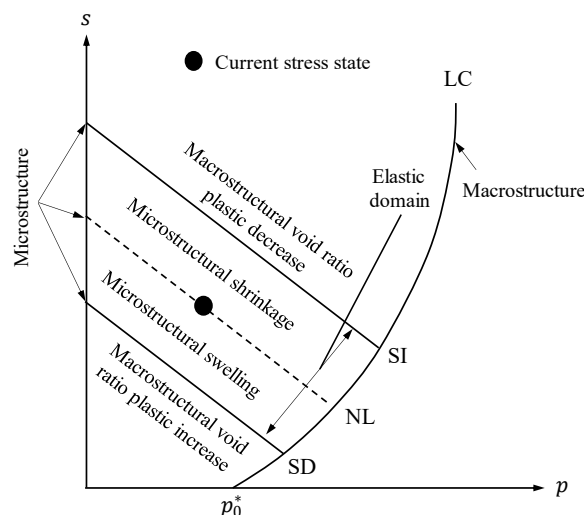


Figure 1. BExM yield loci in  $p$ - $s$  plane.

The behavior of the macrostructure is defined based on the load-collapse (LC) yield surface. When the stress path intersects this yield surface, irreversible volumetric strains in the macrostructure occur. For the triaxial stress state, the deviatoric stress variable is utilized. The model is based on the Modified Cam-Clay model. Hence, the three-dimensional yield curve can be illustrated, as shown in Figure 2.

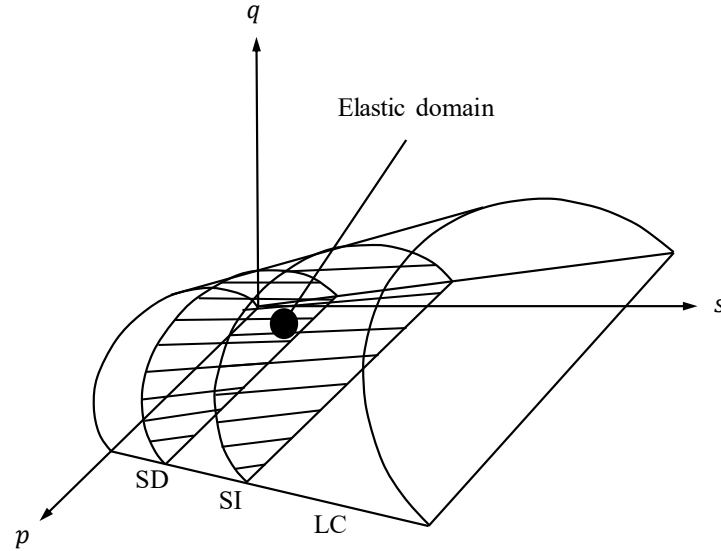


Figure 2. BExM yield loci in  $p$ - $q$ - $s$  space.

In this three-dimensional space, the yield curve (LC) is defined by the following equation:

$$q^2 - M^2(p + k_s s)(p_0 - p) = 0 \quad (1)$$

where  $M$  is the slope of the critical state line,  $k_s$  is the cohesion increment parameter with suction, and  $p_0$  is the preconsolidation stress at the specific suction  $s$ , which defines the shape of the yield curve (LC) on the  $p$ - $s$  plane and is expressed as follows:

$$p_0 = p_c \left[ \frac{p_0^*}{p_c} \right]^{\frac{\lambda(0)-\kappa}{\lambda(s)-\kappa}} \quad (2)$$

$$\lambda(s) = \lambda(0) [r + (1-r)e^{-\beta s}] \quad (3)$$

where  $p_0^*$  is the saturated preconsolidation pressure,  $p_c$  is a reference pressure,  $\lambda(0)$  is the slope of the virgin saturated consolidation line,  $\lambda(s)$  is the slope of the virgin consolidation line at suction  $s$ ,  $\kappa$  is the slope of the unloading-reloading line in  $e$ - $\ln(p)$  diagram,  $r$  is a parameter defining the maximum soil stiffness, and  $\beta$  is a parameter controlling the increase rate of soil stiffness with suction. SI and SD yield surfaces are taken parallel to NL and are expressed respectively as:

$$\hat{p} - s_i = 0 \quad (4)$$

$$s_0 - \hat{p} = 0 \quad (5)$$

where  $s_i$  and  $s_0$  are hardening parameters. It was assumed that SI and SD hardenings are governed by  $d\alpha_1 = d\varepsilon_{vSI}^p + d\varepsilon_{vSD}^p$  where  $d\varepsilon_{vSI}^p$  and  $d\varepsilon_{vSD}^p$  are the volumetric plastic strains due to activation of respectively SI and SD. Macrostructural yield surface (LC) hardening is assumed to depend on  $d\alpha_2 = d\varepsilon_{vSI}^p + d\varepsilon_{vSD}^p + d\varepsilon_{vLC}^p$  where  $d\varepsilon_{vLC}^p$  is the volumetric plastic strain due to the activation of LC. Hardening laws are defined as follows:

$$ds_i = \frac{K_m d\alpha_1}{f} = ds_0 \quad (6)$$



$$\frac{dp_0^*}{p_0^*} = \frac{(1 + e_M)d\alpha_2}{\lambda(0) - \kappa} \quad (7)$$

where  $K_m$  is the microstructural bulk modulus for changes in suction plus mean stress,  $e_M$  is the macrostructural void ratio, and the function  $f$  corresponds to the micro and macrostructural coupling function, that is  $f = f_I$  if SI is active and  $f = f_D$  if SD is active. These coupling functions are defined as:

$$f_D = f_{D0} + f_{D1} \left(1 - \frac{p}{p_0}\right)^{n_D} \quad (8)$$

$$f_I = f_{I0} + f_{I1} \left(\frac{p}{p_0}\right)^{n_I} \quad (9)$$

where  $f_{D0}$ ,  $f_{D1}$ ,  $n_D$ ,  $f_{I0}$ ,  $f_{I1}$ , and  $n_I$  are model parameters.

### 3. Soil type and model parameters

Various studies have explored wetting and drying cycles on different types of soils. [Alonso et al. \(1999\)](#) conducted studies on a type of expansive clay known as Boom clay. [Alonso et al. \(2005\)](#) used a mixture of silica sand and calcium-bentonite powder in proportions of 20 to 80 percent, respectively. Additionally, [Lloret et al. \(2003\)](#) studied a specific bentonite type in southeastern Spain, comprising over 90 percent of montmorillonite minerals. Furthermore, [Noamouz et al. \(2009\)](#) investigated a type of clay in the Le Deffend region of France. In this study, parameters from Boom clay originating in Belgium, as reported by [Sanchez et al. \(2005\)](#), shown in [Table 1](#). According to the Unified Soil Classification System, Boom clay is an inorganic, high-plasticity type of clay, with a liquid limit ranging from 23 to 29 percent, a plastic limit from 55 to 80 percent, and a plasticity index from 32 to 51 percent.

### 4. Hydro-mechanical model

For the one-dimensional modeling of wetting-drying cycles, a soil column 10 m in height and 1 m in width was considered. [Figure 3](#) illustrates the boundary conditions and finite element discretization using quadrilateral four-node elements. The soil column was constrained against horizontal displacement at the vertical boundary and against vertical displacement at the bottom boundary. To simulate wetting and drying cycles, suction was applied at the upper boundary at different intervals. Additionally, surcharges of 10 and 20 kPa were applied at this boundary, separately. The model properties are presented in [Table 2](#). A total of six wetting and drying cycles were chosen for all models, following [Alonso et al. \(2005\)](#). Initially, the soil column was subjected to loading for one day until reaching its initial equilibrium suction, as a first time step. Subsequently, the column underwent reduced suction, initiating the wetting process. Each wetting and drying path lasted for 20 days. At the end of the 21st day, the soil column was subjected to increased suction, commencing the drying process. After 41 days, the first cycle is finished, and the subsequent cycle is commenced.

As a result of moisture variations caused by changes in suction along wetting and drying paths, the volume of soil undergoes alterations in both macrostructure and microstructure levels. These volumetric changes manifest cyclic deformations. In wetting paths, the soil swells due to increased moisture (reduced suction). Conversely, in drying paths, the soil shrinks as moisture decreases (increased suction).

In Models 1 and 2, an initial suction of 50 MPa was applied, while in Models 3 and 4, an initial suction of 80 MPa was assigned. The initial path was a wetting path, and the models reached a minimum suction of 5 MPa at the end of this path. Subsequently, at the end of the drying path, the models returned to their maximum suctions of 50 and 80 MPa, respectively. A microstructure void ratio of 0.2 and a macrostructure void ratio of 0.5 were assigned to the soil domain. An initial preconsolidation pressure in a saturated state ( $p_0^*$ ) of 0.1 MPa was considered as an initial condition of the soil column.



**Table 1. Input parameters of the mechanical constitutive model.**

| Parameter                 | Description   | Value |
|---------------------------|---|-------|
| <b>Elastic Model</b>      |   |       |
| $\kappa^{Macro}$          | Matrix elastic stiffness parameter at macro level for changes in mean stress ( $p$ )                        | 0.02  |
| $\kappa^{micro}$          | Matrix elastic stiffness parameter at micro level for changes in mean effective stress, ( $p + s^{micro}$ ) | 0.1   |
| $\kappa_s$                | Elastic macro stiffness parameter for changes in macro suction ( $s^{macro}$ )                              | 0.01  |
| $\nu^M$                   | Poisson's ratio   | 0.3   |
| $K_{min}^{Macro}$         | Minimum bulk modulus at macro level (MPa)   | 0.001 |
| $K_{min}^{micro}$         | Minimum bulk modulus at micro level (MPa)   | 0.001 |
| <b>Coupling Behaviour</b> |   |       |
| $f_{sd0}$                 |   | -0.1  |
| $f_{sd1}$                 | Micro and macrostructure coupling functions when SD is activated  | 1.1   |
| $n_{sd}$                  |   | 2     |
| $f_{si0}$                 |   | -0.1  |
| $f_{si1}$                 | Micro and macrostructure coupling functions when SI is activated  | 1.1   |
| $n_{si}$                  |   | 0.5   |
| <b>Yield Surface</b>      |   |       |
| $M$                       | Slope of the critical state line  | 1     |
| $r$                       | Coefficient setting the change in cohesion with suction   | 0.78  |
| $\beta$                   | Coefficient setting the change in cohesion with suction (MPa <sup>-1</sup> )                                | 5     |
| $p_c$                     | Reference pressure (MPa)  | 0.01  |
| $k_s$                     | Coefficient setting the increase of tensile strength with suction   | 0     |
| $p_{t0}$                  | Cohesion corresponding to suction equal to zero (MPa)   | 0.01  |
| $p_0^*$                   | Preconsolidation mean stress for saturated soil (MPa)   | 0.1   |
| <b>Plastic Potential</b>  |   |       |
| $\omega$                  | Coefficient of nonassociativity   | 1     |
| <b>Hardening Law</b>      |   |       |
| $\lambda(0)$              | Slope of the virgin loading line in the $e-\ln(p)$ diagram  | 0.65  |

**Table 2. Model properties.**

| Name    | Suction range (MPa) | Surcharge (kPa) |
|---------|---------------------|-----------------|
| Model 1 | 5 – 50              | 10              |
| Model 2 | 5 – 50              | 20              |
| Model 3 | 5 – 80              | 10              |
| Model 4 | 5 – 80              | 20              |

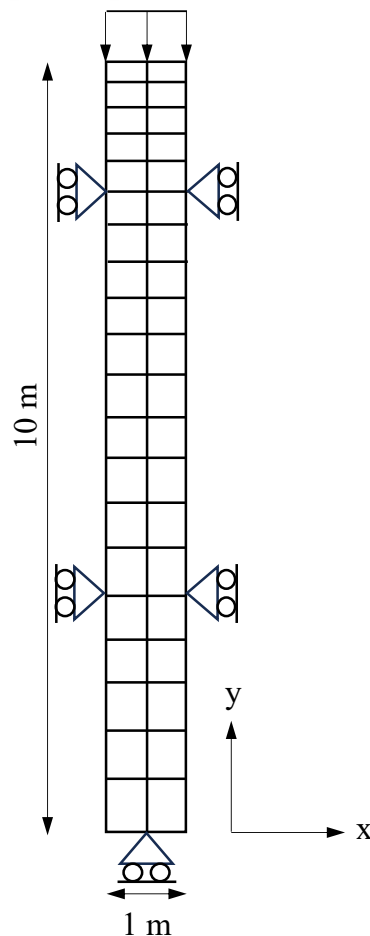


Figure 3. One-dimensional homogeneous soil column with finite element mesh.

## 5. Results and discussion

The vertical displacement of the soil column against wetting and drying cycles under 10 and 20 kPa surcharges was depicted in Figure 4, where the first path in each cycle represents the wetting (straight lines) and the second path represents drying (dashed lines). Upward deformations indicate soil expansion, while downward deformations represent soil shrinkage. As shown in Figure 3, the deformations' range is greater in the higher suction range (from 5 to 80 MPa) compared to the lower suction range (from 5 to 50 MPa). As the applied surcharge increases, the soil's tendency to exhibit swelling diminishes, and the soil reaches equilibrium after fewer wetting and drying cycles. At equilibrium, the volumetric expansion in the wetting path equals the shrinkage in the drying path, signifying cumulative deformation is about zero. The soil exhibits elastic behavior at this point, with the swelling deformation observed in the wetting path returning to its previous state by the end of the drying path.

Under lower surcharge (10 kPa), the initial swelling is the highest, and the difference between swelling and shrinkage is representative of the plastic deformation. Over several cycles, these deformations decrease until they nearly approach zero, indicating elastic behavior in the soil. This pattern differs under higher surcharge (20 kPa), where the soil initially demonstrates nearly elastic behavior in the first cycles, followed by the onset of plastic behavior after a few cycles. As the surcharge range increases, the number of initial elastic cycles rises. This behavior has also been reported by Estabragh et al. (2014) for higher surcharge conditions.

Due to moisture changes resulting from alterations in stress, both the macro and microstructural properties of the soil change. Among the key soil parameters, the dry density variation during wetting and drying cycles under surcharges of 10 and 20 kPa are illustrated in Figure 5. The dry density decreases from its initial value of 1350 kg/m<sup>3</sup> to approximately 950 kg/m<sup>3</sup>. Wetting and drying cycles have a decreasing effect on dry density, primarily due to increased pore volume and soil expansion leading to decreased dry density. Although in the drying paths, volume reduction and increased dry density occur due to soil shrinkage, the dominant factor is swelling deformation, resulting in decreased dry density by the end of six wetting and drying

cycles. The surcharge has an increasing effect on dry density, where an increase in surcharge leads to reduced swelling and increased soil density. Higher variations in dry density are observed with an increase in suction levels. In the last wetting path, under a suction range of 5 to 50 MPa at 10 kPa surcharge, the minimum dry density is around 985 kg/m<sup>3</sup>, while at a suction range of 5 to 80 MPa under the same 10 kPa surcharge, the minimum dry density is approximately 931 kg/m<sup>3</sup>.

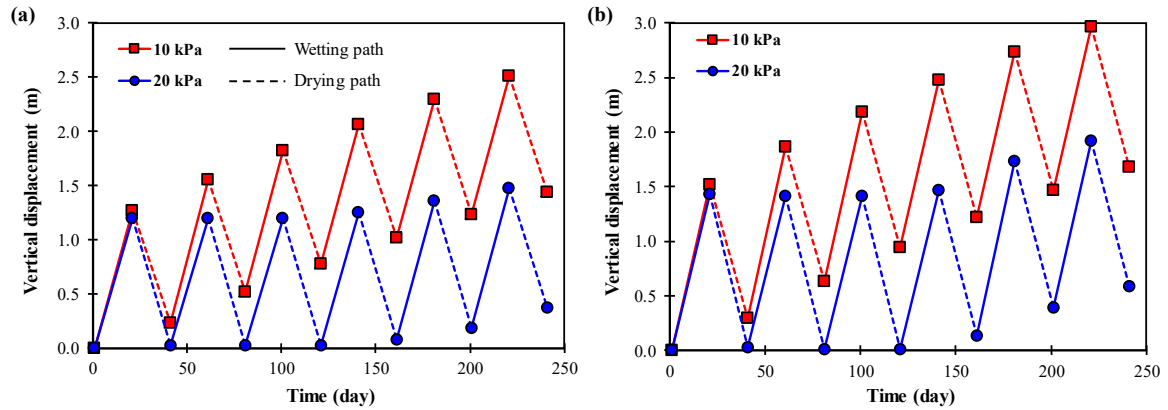


**Figure 4. Vertical displacement of soil column during wetting and drying cycles, (a) suction range of 5 – 50 MPa and (b) suction range of 5 – 80 MPa**

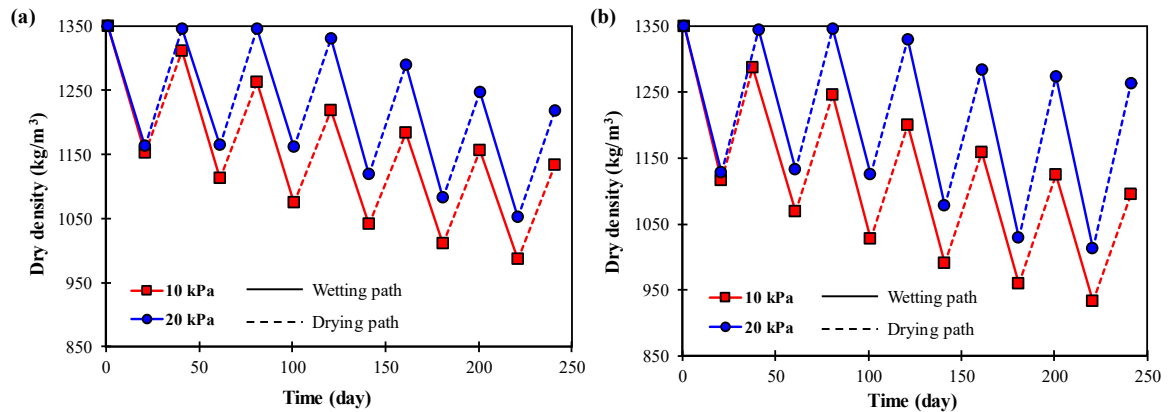


**Figure 5. Variations of the dry density during wetting and drying cycles, (a) suction range of 5 – 50 MPa and (b) suction range of 5 – 80 MPa**

Figure 6 illustrates variations in porosity-suction during wetting and drying paths. The trends observed in these variations are similar to the vertical displacement patterns shown in Figure 4. Figure 6 (b) and (d) display porosity variations under higher surcharge, highlighting that in the first wetting and drying paths, minimal porosity changes occur during the cycles. This trend emphasizes the soil's distinct response under higher surcharge conditions. Additionally, it is apparent that under higher surcharges, the soil behavior transitions successively from elastic to plastic and back to elastic behavior. This behavior becomes more pronounced in the higher range of suction variations, as depicted in Figure 6 (c).



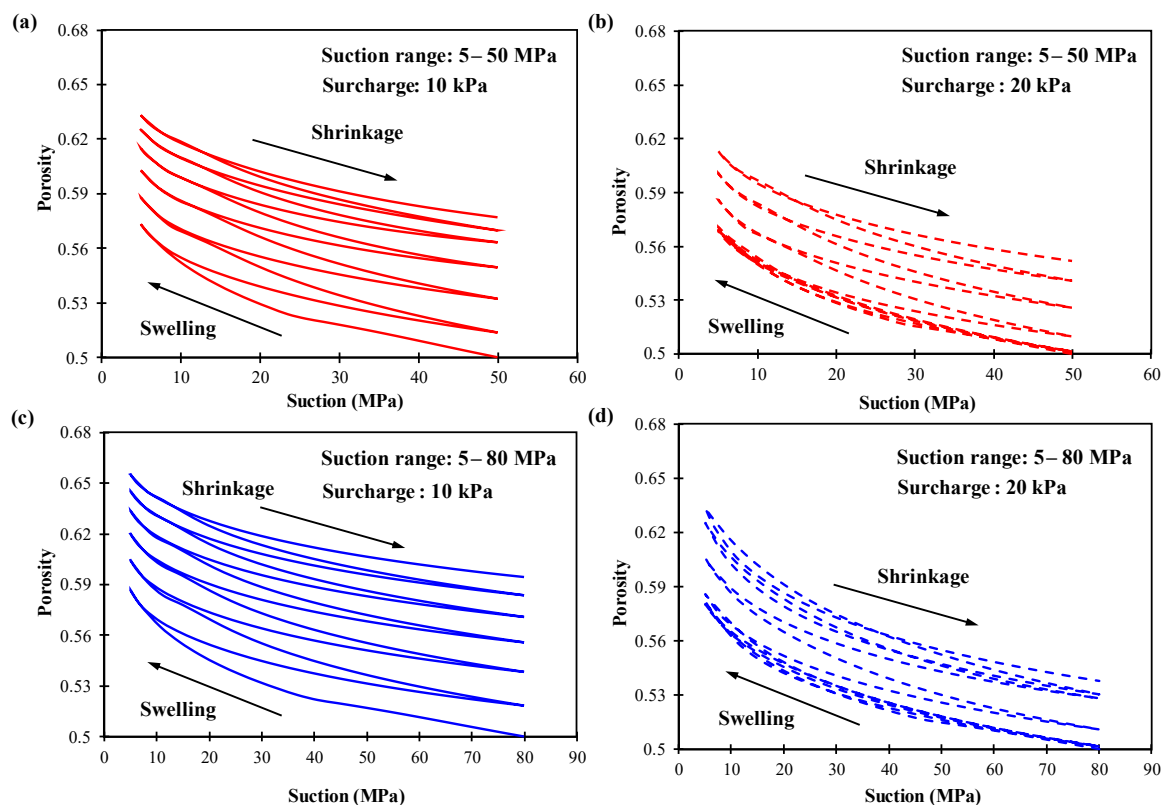


**Figure 6.** Variations of porosity-suction, (a) suction range: 5 – 50 MPa and surcharge: 10 kPa, (b) suction range: 5 – 50 MPa and surcharge: 20 kPa, (c) suction range: 5 – 80 MPa and surcharge: 10 kPa, (d) suction range: 5 – 80 MPa and surcharge: 20 kPa

## 6. Conclusions

This study employed the Barcelona Expansive Model (BExM) as a theoretical framework for numerical modeling, defining the coupled hydro-mechanical analyses observed in experiments on swelling unsaturated soils. The model was implemented using the finite element program CODE\_BRIGHT. This model effectively represents the stress-path dependency of the swelling and shrinkage behavior of unsaturated expansive soils. It also accounts for the correlation between microstructural and macrostructural behavior in soil volumetric deformations. The investigation assessed the influence of suction variations in stress increments of 10 and 20 kPa across four scenarios. The results indicated that in wetting paths, due to moisture changes and soil suction alterations, there is an increase in soil volume within the microstructure, leading to particle arrangement changes in the macrostructure, eventually resulting in irreversible void ratio changes. Conversely, in drying paths, there is a reduction in the microstructure's volume, leading to irreversible void ratio reduction. This trend was illustrated through vertical displacement of the soil column, dry density over time, and porosity-suction variations. Initially, the expansive soil experienced substantial volume changes in the primary cycles, gradually reaching equilibrium after several wetting and drying cycles, showing elastic and reversible deformations. Furthermore, the study revealed that with higher surcharges, the soil behavior differed, and plastic strains did not necessarily occur in the initial cycles.

## 7. References

1. Alonso, E. E., Romero, E., Hoffmann, C., & García-Escudero, E. (2005). Expansive bentonite-sand mixtures in cyclic controlled-suction drying and wetting. *Engineering Geology*, 81(3), 213–226. <https://doi.org/10.1016/j.enggeo.2005.06.009>
2. Alonso, E. E., Vaunat, J., & Gens, A. (1999). Modelling the mechanical behaviour of expansive clays. In *Engineering Geology* (Vol. 54). [https://doi.org/10.1016/S0013-7952\(99\)00079-4](https://doi.org/10.1016/S0013-7952(99)00079-4)
3. Alonso, E.E., Gens, A. and Josa, A., 1990. A constitutive model for partially saturated soils. *Géotechnique*, 40(3), pp.405-430. <https://doi.org/10.1680/geot.1990.40.3.405>



4. Estabragh, A. R., Parsaei, B., & Javadi, A. A. (2015). Laboratory investigation of the effect of cyclic wetting and drying on the behaviour of an expansive soil. *Soils and Foundations*, 55(2), 304–314. <https://doi.org/10.1016/j.sandf.2015.02.007>
5. Ghandilou, M.J., Turchi, S. and Sadeghi, H., 2023, June. Numerical Investigation of Cyclic Wetting and Drying of Boom Clay Based on the Barcelona Expansive Model. In 84th EAGE Annual Conference & Exhibition (Vol. 2023, No. 1, pp. 1-5). European Association of Geoscientists & Engineers. <https://doi.org/10.3997/2214-4609.202310400>
6. Jabbarzadeh, M., Sadeghi, H., Turchi, S. and Darzi, A.G., 2023. Thermo-hydraulic analysis of desiccation cracked soil strata considering ground temperature and moisture dynamics under the influence of soil-atmosphere interactions. <https://doi.org/10.31223/X58Q38>
7. Lloret, A., Villar, M.V., Sanchez, M., Gens, A., Pintado, X. and Alonso, E.E., 2003. Mechanical behaviour of heavily compacted bentonite under high suction changes. *Géotechnique*, 53(1), pp.27-40. <https://doi.org/10.1680/geot.2003.53.1.27>
8. Mrad, M., Abdallah, A., Masrouri, F., Vaunat., J. (2006). Finite-Element implementation of BExM elastoplastic model for swelling unsaturated soils. In *ASCE*. [https://doi.org/10.1061/40802\(189\)163](https://doi.org/10.1061/40802(189)163)
9. Nowamooz, H., Mrad, M., Abdallah, A., & Masrouri, F. (2009). Experimental and numerical studies of the hydromechanical behaviour of a natural unsaturated swelling soil. *Canadian Geotechnical Journal*, 46(4), 393–410. <https://doi.org/10.1139/T08-127>
10. Olivella, S., Gens, A., Carrera, J., & Alonso, E. E. (1996). Numerical formulation for a simulator (CODE\_BRIGHT) for the coupled analysis of saline media. *Engineering Computations (Swansea, Wales)*, 13(7), 87–112. <https://doi.org/10.1108/02644409610151575>
11. Qi, S., & Vanapalli, S. K. (2015). Hydro-mechanical coupling effect on surficial layer stability of unsaturated expansive soil slopes. *Computers and Geotechnics*, 70, 68–82. <https://doi.org/10.1016/j.compgeo.2015.07.006>
12. Sadeghi, H., Kohal, F.Y.B., Gholami, M., Alipanahi, P. and Song, D., 2023. Hydro-mechanical modeling of a vegetated slope subjected to rainfall. In *E3S Web of Conferences* (Vol. 382, p. 13004). EDP Sciences. <https://doi.org/10.1051/e3sconf/202338213004>
13. Sánchez, M., Gens, A., do Nascimento Guimarães, L., & Olivella, S. (2005). A double structure generalized plasticity model for expansive materials. *International Journal for Numerical and Analytical Methods in Geomechanics*, 29(8), 751–787. <https://doi.org/10.1002/nag.434>
14. Wen, T., Chen, X. and Shao, L., 2022. Effect of multiple wetting and drying cycles on the macropore structure of granite residual soil. *Journal of Hydrology*, 614, p.128583. <https://doi.org/10.1016/j.jhydrol.2022.128583>
15. Xu, X.T., Liu, D.Q., Xian, Z.X., Yang, F., Jian, W.B., Xu, X. and Huang, J.B., 2022. Influence of Drying–Wetting Cycles on the Water Retention and Microstructure of Residual Soil. *Geofluids*, 2022. <https://doi.org/10.1155/2022/9948658>
16. Zhao, N.F., Ye, W.M., Chen, B., Chen, Y.G. and Cui, Y.J., 2019. Modeling of the swelling–shrinkage behavior of expansive clays during wetting–drying cycles. *Acta Geotechnica*, 14, pp.1325-1335. <https://doi.org/10.1007/s11440-018-0718-6>